Spontaneous Isomerization of Symmetric M(μ-NO)$_2$M Linkages to (ON)M=N=M=O Groupings

Peter Legzdins,*,† Michelle A. Young,† Raymond J. Batchelor,‡ and Frederick W. B. Einstein*,‡

Contribution from the Departments of Chemistry, The University of British Columbia, Vancouver, British Columbia, Canada V6T 1Z1, and Simon Fraser University, Burnaby, British Columbia, Canada V5A 1S6

Received November 16, 1994. Revised Manuscript Received June 23, 1995[⊗]

Abstract: Treatment of Cp*Mo(NO)R$_2$ complexes (Cp* = η^5-C$_5$Me$_5$; R = CH$_2$CMe$_3$, CH$_2$CMe$_2$Ph) in C$_6$H$_6$ at 5 °C with H$_2$ results in the formation of [Cp*MoR]$_2$(μ-NO)$_2$ products (R = CH$_2$CMe$_3$ (**1**), CH$_2$CMe$_2$Ph (**2**)) which are isolable in 25−30% yields. Similar treatment of an equimolar mixture of Cp*Mo(NO)(CH$_2$SiMe$_3$)$_2$ and Cp*W(NO)(CH$_2$SiMe$_3$)$_2$ with H$_2$ results in the formation of a heterobimetallic species, [Cp*Mo(CH$_2$SiMe$_3$)](μ-NO)$_2$[Cp*W(CH$_2$SiMe$_3$)] (**3**). Complexes **1**, **2**, and **3** isomerize in solution at ambient temperatures to form [Cp*Mo(NO)R](μ-N)[Cp*Mo(O)R] (R = CH$_2$CMe$_3$ (**4**), CH$_2$CMe$_2$Ph (**5**)) and a 60:40 (M$_1$ = W:M$_1$ = Mo) mixture of [Cp*M$_1$(NO)(CH$_2$SiMe$_3$)](μ-N)[Cp*M$_2$(O)(CH$_2$SiM$_3$)] (**6**), respectively. The solid-state molecular structures of **1** and **6** have been established by single-crystal X-ray crystallographic analyses. Crystals of [Cp*Mo(CH$_2$CMe$_3$)]$_2$(μ-NO)$_2$ (**1**) are orthorhombic of space group *Pbcn*: a = 12.570(3) Å, b = 15.566(2) Å, c = 15.610(3) Å, Z = 4, V = 3054.3 Å^3, T = 185 K, R_f = 0.025 for 1921 data ($I_o \geq 2.5\sigma(I_o)$) and 196 parameters. Crystals of [Cp*M$_1$(NO)(CH$_2$SiMe$_3$)](μ-N)[Cp*M$_2$(O)(CH$_2$SiMe$_3$)] (polymorph **6B**) are monoclinic of space group $P2_1/c$: a = 13.940(3) Å, b = 19.953(3) Å, c = 12.112(3) Å, β = 97.99(2)°, Z = 4, V = 3336.2 Å^3, T = 297 K, R_f = 0.029 for 3096 data ($I_o \geq 2.5\sigma(I_o)$) and 333 parameters. The most chemically interesting features of the molecular structures of **1** and **6** are the relatively short Mo−Mo single-bond distance of 2.5930 (7) Å in **1** and the nearly linear M−N−M′ multiply bonded arrangement of 157.3(4) in **6**. A kinetic analysis of the isomerization of **2** to **4** in toluene reveals it to be first order in **2** with k_{obsd} (20 °C) = (1.1 ± 0.3) × 10^{-4} s^{-1}. Furthermore, kinetic analysis at various temperatures establish that $\Delta H^{\ddagger}$ = 39 ± 3 kJ/mol and $\Delta S^{\ddagger}$ = −188 ± 6 J/mol K (−45 ± 3 cal/mol K), values consistent with the isomerization occurring in an intramolecular manner. A plausible mechanism for the spontaneous isomerization of the symmetric M(μ-NO)$_2$M linkages to the (ON)M=N=M=O groupings is proposed.

Introduction

Cleavage of the N−O bond is metal-bound nitric oxide is both of fundamental significance in inorganic chemistry and of relevance to biological and environmental chemistry.[1] Such NO activation has to date been reported to occur in several monometallic and polymetallic systems. For example, it occurs during the gas-phase ion chemistry of metal clusters[2] as well as during some of their transformations in the condensed phase.[3] Furthermore, the degradation of the dinitrosyl complex CpCr(NO)$_2$Cl (Cp = η^5-C$_5$H$_5$) monitored by mass spectroscopy has revealed fragmentation patterns consistent with nitrosyl N−O bond cleavage.[4] More recently, tandem mass spectrometry has demonstrated that Cp$_2$Fe$_2$(NO)$^+$ undergoes N−O bond cleavage, the resulting fragments being pyridine and CpFe$_2$O$^+$.[5] Finally, there have also been reports of the Lewis-acid-induced conversion of terminal nitrosyl ligands into terminal oxo and nitrido groups,[6] and nitrosyl metal clusters have been shown to undergo dissociation of nitrosyl N−O bonds to afford nitrido clusters.

During our continuing studies with organometallic nitrosyl complexes of the group 6 elements, we have generally found that the NO ligand remains intact during various reactions involving these compounds. However, a new kind of reactivity that we are encountering with ever increasing frequency with these systems is that of nitrosyl N−O bond cleavage.[8] One of the first such processes discovered in our group was the water-catalyzed isomerization of the diarly nitrosyl complex CpW(NO)(*o*-tolyl)$_2$ into the oxo imido species CpW(*o*-tolyl)(O)(N-*o*-tolyl), which we reported in 1991.[9] Subsequently we discovered that the thermolysis of Cp*W(NO)Ph$_2$ (Cp* = η^5-C$_5$Me$_5$) affords the N−O bond dissociated products Cp*(NO)(η^2-ON-Ph)(NPh)Ph and [Cp*W(O)Ph](μ-N)[Cp*W(NO)Ph].[10] Very recently, we reported that treatment of Cp*Mo(NO)(CH$_2$SiMe$_3$)$_2$ in benzene with molecular hydrogen at ambient temperatures leads to the formation of the bimetallic nitrido-bridged complex [Cp*Mo(NO)(CH$_2$SiMe$_3$)](μ-N)[Cp*Mo(O)(CH$_2$SiMe$_3$)], as sum-

† The University of British Columbia.
‡ Simon Fraser University.
[⊗] Abstract published in *Advance ACS Abstracts*, August 1, 1995.

(1) (a) Sadler, P. J. *Adv. Inorg. Chem.* **1991**, *36*, 1. (b) Kummer, J. T. *J. Phys. Chem.* **1986**, *90*, 4747. (c) Legzdins, P.; Rettig, S. J.; Sayers, S. F. *J. Am. Chem. Soc.* **1994**, *116*, 12105 and references cited therein.
(2) (a) Fredeen, D. J. A.; Russell, D. H. *J. Am. Chem. Soc.* **1986**, *108*, 1860. (b) Jacobson, D. B. *J. Am. Chem. Soc.* **1987**, *109*, 6851. (c) Klaassen, J. J.; Jacobson, D. B. *J. Am. Chem. Soc.* **1988**, *110*, 974. (d) Gord, J. R.; Freiser, B. S. *J. Am. Chem. Soc.* **1989**, *111*, 3754.
(3) (a) Gland, J. L.; Sexton, B. A. *Surf. Sci.* **1980**, *94*, 355. (b) Baldwin, E. K.; Friend, C. M. *J. Phys. Chem.* **1985**, *89*, 2576.
(4) Müller, J.; Lüdemann, F.; Schmitt, S. *J. Organomet. Chem.* **1979**, *169*, 25.
(5) Schröder, D.; Müller, J.; Schwarz, H. *Organometallics* **1993**, *12*, 1972.
(6) Seyferth, K.; Taube, R. *J. Mol. Catal.* **1985**, *28*, 53.
(7) (a) Gladfelter, W. L. *Adv. Organomet. Chem.* **1985**, *24*, 41. (b) Gibson, C. P.; Dahl, L. F. *Organometallics* **1988**, *7*, 543. (c) Gibson, C. P.; Bern, D. S.; Falloon, S. B.; Hitchens, T. K.; Cortopassi, J. E. *Organometallics* **1991**, *10*, 1742. (d) Feasey, N. D.; Knox, S. A. R. *J. Chem. Soc., Chem. Commun.* **1982**, 1063.
(8) Legzdins, P.; Young, M. A. *Comments Inorg. Chem.* **1995**, *17*, 239.
(9) Legzdins, P.; Rettig, S. J.; Ross, K. J.; Veltheer, J. E. *J. Am. Chem. Soc.* **1991**, *113*, 4361.
(10) Brouwer, E. B.; Legzdins, P.; Rettig, S. J.; Ross, K. J. *Organometallics* **1994**, *13*, 2088.

0002-7863/95/1517-8798$09.00/0

Table 1. Numbering Scheme, Color, Yield, and Elemental Analysis Data

complex	compd no.	color (yield, %)	anal. found (calcd) C	H	N
$[Cp^*Mo(CH_2CMe_3)]_2(\mu\text{-}NO)_2$	**1**	blue (26)	54.42 (54.20)	8.03 (7.90)	4.23 (4.21)
$[Cp^*Mo(CH_2CPhMe_2)]_2(\mu\text{-}NO)_2$	**2**	blue (33)	60.67 (60.90)	7.10 (7.17)	3.40 (3.55)
$[Cp^*Mo(CH_2SiMe_3)](\mu\text{-}NO)_2[Cp^*W(CH_2SiMe_3)]$	**3**	blue (30)	42.85 (42.85)	6.74 (6.69)	3.45 (3.57)
$[Cp^*Mo(NO)(CH_2CMe_3)](\mu\text{-}N)[Cp^*Mo(O)(CH_2CMe_3)]$	**4**	brown (>95)[b]	54.03 (54.20)	7.83 (7.90)	4.03 (4.21)
$[Cp^*Mo(NO)(CH_2CPhMe_2)](\mu\text{-}N)[Cp^*Mo(O)(CH_2CPhMe_2)]$	**5**	brown (>95)[b]	61.07 (60.90)	7.23 (7.17)	3.53 (3.55)
$[Cp^*M_1(NO)(CH_2SiMe_3)](\mu\text{-}N)[Cp^*M_2(O)(CH_2SiMe_3)]$[a]	**6**	brown-red (>95)[b]	42.87 (42.85)	6.86 (6.69)	3.57 (3.57)

[a] A mixture of isomers: M_1 = W (60%); M_1 = Mo (40%). [b] By ^1H NMR (based on the corresponding bimetallic bridging NO precursor).

Table 2. Mass Spectral and Infrared Data

compd no.	MS (*m/z*)[b]	temp[a] (°C)	IR (Nujol mull) ν_{NO}	other strong bands
1	664 [P^+]	100	1332 (vs)	
2	788 [P^+]	120	1339 (vs)	
3	784 [P^+]	150	1314 (brd)	950, 930, 909, 845, 829
4	664 [P^+]	100	1591 (vs)	919, 841
5	788 [P^+]	120	1592 (vs)	919, 842, 801
6	784 [P^+]	150	1576, 1555 (brd)	997, 978, 956, 933, 917

[a] Probe temperatures. [b] Values for the highest intensity peak of the calculated isotopic cluster (^{96}Mo and ^{184}W).

marized in eq. 1.[11] At the time we proposed that this bimetallic

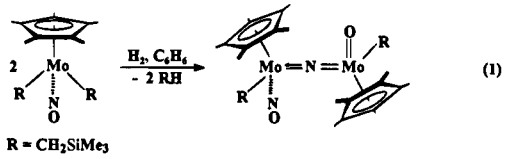

(1)

product probably results via the transient formation of the coordinatively unsaturated $Cp^*Mo(\eta^2\text{-}NO)(CH_2SiM_3)$ intermediate that then combines with another molecule of the original $Cp^*Mo(NO)(CH_2SiMe_3)_2$ reactant. However, as we attempted to extend conversion 1 to encompass the related bis(neopentyl) and bis(neophyl) complexes of molybdenum, we discovered, and now wish to report, that the initially formed intermediates are actually the symmetric $[Cp^*Mo(R)]_2(\mu\text{-}NO)_2$ (R = alkyl) bimetallic species which then undergo an unprecedented spontaneous isomerization to the final nitrido-bridged products.

Experimental Section

All reactions and subsequent manipulations were performed under anaerobic and anhydrous conditions using an atmosphere of prepurified argon. General procedures routinely employed in our laboratories have been described in detail previously.[12] All weighings were performed on a Mettler AE-166 analytical balance. The organometallic reagents, namely $Cp^*M(NO)Cl_2$ (M = Mo, W)[13] and $Cp^*Mo(NO)(CH_2SiMe_3)_2$,[14] were prepared by reported procedures. $Cp^*Mo(NO)(CH_2CMe_3)_2$, $Cp^*Mo(NO)(CH_2CMe_2Ph)_2$, and $Cp^*W(NO)(CH_2SiMe_3)_2$ have all been previously prepared;[15] however, details of their preparation and characterization data have been included in this Experimental Section. The organomagnesium reagents, namely $(Me_3CCH_2)_2Mg\cdot x(dioxane)$[16] and $(Me_2PhCCH_2)_2Mg\cdot x(dioxane)$,[14] were prepared by their published procedures. H_2 (Linde, extra dry) and $(Me_3SiCH_2)MgCl$ (1.0 M in Et_2O, Aldrich) were used as received. Acetone and benzaldehyde (Fisher) were dried on CaH_2 and distilled before use. The column chromatographic material employed during this work was Florisil (60−100 mesh, Fisher). Filtrations were performed through Celite 545 diatomaceous earth (Fisher) or alumina I (Fisher, neutral) that had been oven-dried and cooled in vacuo. Spectroscopic data, yields, and elemental analyses of all new complexes synthesized during this work are collected in Tables 1−3.

Preparation of $Cp^*Mo(NO)(CH_2CMe_3)_2$ and $Cp^*Mo(NO)(CH_2CMe_2Ph)_2$. Both of these complexes were prepared in a similar manner, and the preparation of $Cp^*Mo(NO)(CH_2CMe_3)_2$ is given as a representative example.

In a glovebox, $Cp^*Mo(NO)Cl_2$ (332 mg, 1.00 mmol) and $(Me_3CCH_2)_2Mg\cdot x(dioxane)$ (330 mg, 1.00 mmol) were weighed into a Schlenk tube. THF (20 mL) was vacuum transferred onto the solids at −196 °C. The stirred reaction mixture was warmed slowly (1 h) to 0 °C, whereupon the reaction mixture turned red. The residue was suspended in Et_2O (30 mL), treated with 2 drops of water, and quickly transferred onto a column of alumina I (2 × 3 cm) supported on a glass frit. The column was washed with Et_2O (20 mL) until the eluate was colorless. The ether was then removed from the filtrate to afford a red powder which was dissolved in a minimum of pentane (5 mL). Cooling of this solution at −30 °C overnight resulted in the formation of red crystals of $Cp^*Mo(NO)(CH_2CMe_3)_2$ (240 mg, 59% yield).

Similarly, $Cp^*Mo(NO)(CH_2CMe_2Ph)_2$ was isolated as red crystals in 70% yield. However, the addition of water was omitted from this procedure.

Anal. Calcd for $C_{20}H_{37}NOMo$: C, 59.54; H, 9.24; N, 3.47. Found: C, 59.70; H, 9.35; N, 3.50. IR (Nujol): ν_{NO} 1593 (vs) cm^{-1}. ^1H NMR (C_6D_6): δ 3.08 (d, 2H, CH_2, J_{HH} = 12.1 Hz), 1.61 (s, 18H, CMe_3), 1.45 (s, 15H, C_5Me_5), −0.95 (d, 2H, CH_2, J_{HH} = 12.1 Hz). Low-resolution mass spectrum (probe temperature 150 °C): *m/z* 405 [P^+].

Anal. Calcd for $C_{30}H_{41}NOMo$: C, 65.64; H, 6.83; N, 3.06. Found: C, 65.89; H, 6.84; N, 3.14. IR (Nujol): ν_{NO} 1594 (vs) cm^{-1}. ^1H NMR (C_6D_6): δ 7.43 (m, 4H, Ph), 7.20 (m, 4H, Ph), 7.09 (m, 2H, Ph), 3.21 (d, 2H, CH_2, J_{HH} = 10.2 Hz), 1.55 (s, 6H, CMe_3), 1.37 (s, 6H, CMe_3), 1.21 (s, 15H, C_5Me5), −0.85 (d, 2H, CH_2, J_{HH} = 10.2 Hz). Low-resolution mass spectrum (probe temperature 100 °C): *m/z* 529 [P^+].

Preparation of $Cp^*W(NO)(CH_2SiMe_3)_2$. To a rapidly stirred suspension of $Cp^*W(NO)Cl_2$ (420 mg, 1.00 mmol) in Et_2O (50 mL), maintained at −60 °C, was added Me_3SiCH_2MgCl (1.9 mL of a 1.0 M Et_2O solution, 1.00 mmol) via syringe. The reaction mixture was warmed slowly to room temperature (2 h). The final red-brown reaction mixture was concentrated (20 mL) and 5 drops of water added to this mixture. The reaction mixture turned purple immediately and was then filtered through Florisil (2 × 3 cm) supported on a medium porisity frit. The Florisil plug was then rinsed with Et_2O (10 mL). The ether was then removed from the filtrate to afford a purple powder which

(11) Debad, J. D.; Legzdins, P.; Reina, R.; Young, M. A.; Batchelor, R. J.; Einstein, F. W. B. *Organometallics* **1994**, *13*, 4315.
(12) Dryden, N. H.; Legzdins, P.; Rettig, S. J.; Veltheer, J. E. *Organometallics* **1992**, *11*, 2583.
(13) Dryden, N. H.; Legzdins, P.; Batchelor, R. J.; Einstein, F. W. B. *Organometallics* **1991**, *10*, 2077.
(14) Legzdins, P.; Lundmark, P. J.; Phillips, E. C.; Rettig, S. J.; Veltheer, J. E. *Organometallics* **1992**, *11*, 2991.
(15) Veltheer, J. E. Ph.D. Dissertation, The University of British Columbia, 1993.
(16) Dryden, N. H.; Legzdins, P.; Trotter, J.; Yee, V. C. *Organometallics* **1991**, *10*, 2857.

Table 3. NMR Data (C_6D_6)

compd no.	^{1}H NMR (δ, ppm)	^{13}C{^{1}H} NMR (δ, ppm)
1	1.68 (s, 15H, C_5Me_5)	112.13 (C_5Me_5)[a]
	1.19 (s, 9H, CH_2CMe_3)	62.49 (CH_2)
	1.13 (brd s, 2H, CH_2)	38.34 (CMe_3)
		35.39 (CMe_3)
		10.21 (C_5Me_5)
2	7.42 (m, 2H, Ph)	155.28, 127.60, 126.05, 124.79 (Ph)[a]
	7.21 (m, 2H, Ph)	112.53 (C_5Me_5)
	7.08 (m, 1H, Ph)	60.97 (CH_2)
	1.60 (s, 15H, C_5Me_5)	43.61 (CMe_2Ph)
	1.46 (s, 2H, CH_2)	33.86 (CMe_2Ph)
	1.34 (s, 6H, CH_2CMe_2Ph)	10.13 (C_5Me_5)
3	1.72, 1.68 (s, 15H, C_5Me_5)	*b*
	1.52, 0.21 (s, 9H, CH_2SiMe_3)	
	0.27, 0.24, 0.01, −0.20 (s, 1H, CH_2)	
4	2.23 (d, 2H, CH_2, J_{HH} = 11.6 Hz)	115.80, 112.44 (C_5Me_5)[a]
	1.86 (s, 15H, C_5Me_5)	87.36, 59.56 (CH_2)
	1.83 (s, 15H, C_5Me_5)	50.49, 38.24 (CMe_3)
	1.34 (s, 9H, CH_2CMe_3)	33.53, 33.45, 33.37 (CMe_3)
	1.16 (s, 9H, CH_2CMe_3)	10.88, 9.87 (C_5Me_5)
	1.04 (d, 2H, CH_2, J_{HH} = 11.6 Hz)	
5	7.59 (m, 2H, Ph)	155.08, 155.07, 129.06, 128.25, 127.87
	7.28 (m, 5H, Ph)	127.80, 125.95, 125.38, 124.92, 124.68 (Ph)[a]
	7.10 (m, 3H, Ph)	115.70, 112.37 (C_5Me_5)
	2.90 (d, 2H, CH_2, J_{HH} = 11.3 Hz)	73.07, 50.62 (CH_2)
	1.78 (s, 15H, C_5Me_5)	44.50, 40.28 (CMe_2Ph)
	1.73 (s, 15H, C_5Me_5)	32.54, 31.50, 29.78 (CMe_2Ph)
	1.47 (s, 6H, CH_2CMe_2Ph)	11.07, 10.46 (C_5Me_5)
	1.45 (s, 6H, CH_2CMe_2Ph)	
	1.30 (d, 2H, CH_2, J_{HH} = 11.3 Hz)	
6	1.89_A, 1.85_B, 1.82_A, 1.80_B (s, 15H, C_5Me_5)[c]	116.08, 115.27, 112.45, 111.37 (C_5Me_5)
	0.41_A, 0.39_B, 0.28_B, 0.26_A (s, 9H, CH_2SiMe_3)	41.04, 28.87, 15.39, 14.97 (CH_2)
	1.27, 0.84, 0.69, 0.10, 0.09, 0.04 (d, 2H, CH_2, J_{HH} = 12.6 Hz)	11.19, 11.13, 10.10 (C_5Me_5)
		3.65, 3.29, 2.73, 2.48 (CH_2SiMe_3)

[a] Recorded in $CDCl_3$. [b] Not recorded. [c] Ratio of isomers 60:40.

was dissolved in a minimum of pentane (5 mL). Cooling of this solution at −30 °C overnight resulted in the formation of purple crystals of $Cp^*W(NO)(CH_2SiMe_3)_2$ (367 mg, 70% yield).

Anal. Calcd for $C_{18}H_{37}NOMoSi_2$: C, 41.30; H, 7.12; N, 2.68. Found: C, 41.03; H, 7.30; N, 2.67. IR (Nujol): ν_{NO} 1572 (vs) cm^{-1}. ^{1}H NMR (C_6D_6): δ 1.54 (d, 2H, CH_2, J_{HH} = 10.9 Hz), 1.51 (s, 15H, C_5Me_5), 0.36 (s, 18H, $SiMe_3$), −1.48 (d, 2H, CH_2, J_{HH} = 10.9 Hz). Low-resolution mass spectrum (probe temperature 120 °C): *m/z* 523 [P^+].

Preparation of [Cp*MoR]$_2$(μ-NO)$_2$ [R = CH_2CMe_3 (1), CH_2CMe_2Ph (2)]. Both of these complexes were prepared in a similar manner, and the preparation of $[Cp^*Mo(CH_2CMe_3)]_2(\mu\text{-}NO)_2$ (**1**) is given as a representative example. A quantity of C_6H_6 (20 mL) was vacuum transferred onto a solid sample of $Cp^*Mo(NO)(CH_2CMe_3)_2$ (405 mg, 1.00 mmol), and then H_2 (1 atm) was introduced into the reaction vessel. The stirred reaction mixture was warmed slowly to room temperature over 20 min, during which time its color changed from red to bright green. The solvent was removed from the final reaction mixture in vacuo, and the resulting green-blue residue was washed with pentane (5 mL). The washed residue was then dissolved in Et_2O (30 mL) and transferred to the top of a Florisil column (2 × 2 cm) made up in Et_2O and supported on a medium-porosity frit. The column was washed with Et_2O (2 × 20 mL). The filtrate was then taken to dryness under reduced pressure, and the remaining residue was redissolved in a minimal amount of toluene. Cooling of the toluene solution at −30 °C overnight induced the formation of blue crystals of **1** (85 mg, 26% yield), which was isolated by removal of the mother liquor by cannulation. Complex **2** was prepared in a similar manner from $Cp^*Mo(NO)(CH_2CMe_2Ph)_2$ and was isolated in 33% yield.

Preparation of [Cp*Mo(CH$_2$SiMe$_3$)](μ-NO)$_2$[Cp*W(CH$_2$SiMe$_3$)] (3). A cold (5 °C) C_6H_6 (20 mL) solution of $Cp^*Mo(NO)(CH_2SiMe_3)_2$ (332 mg, 0.76 mmol) and $Cp^*W(NO)(CH_2SiMe_3)_2$ (399 mg, 0.76 mmol) was exposed to H_2 (1 atm). The stirred reaction mixture was warmed slowly to room temperature (20 min) during which time its color changed form purple to blue. The solvent was removed from the final reaction mixture in vacuo. The resulting blue powder was then washed with Et_2O (2 × 10 mL) and dried in vacuo. The powder thus obtained was not recrystallized since it was found to be analytically pure **3** (181 mg, 30% yield).

Preparation of [Cp*Mo(NO)(R)](μ-N)[Cp*Mo(O)(R)] [R = CH_2CMe_3 (4), CH_2CMe_2Ph (5)]. Both of these bimetallic complexes were prepared in a similar manner, and the preparation of **4** is given as a representative example. A stirred toluene or Et_2O solution (20 mL) of $[Cp^*Mo(CH_2CMe_3)_2]_2(\mu\text{-}NO)_2$ (**1**) (100 mg, 0.14 mmol) was left at room temperature overnight, whereupon it underwent a color change from blue to brown. The brown solution was then taken to dryness in vacuo. The brown residue was suspended in pentane (20 mL) and filtered through Florisil (2 × 2 cm) supported on a medium-porosity frit. Cooling of the concentrated filtrate at −30 °C for at least 4−6 weeks resulted in the precipitation of **4** as a brown, analytically pure powder.

Complex **5** was prepared similarly from **2**. ^{1}H NMR spectroscopic monitoring of the conversions of **1** → **4** and **2** → **5** in deuterated solvents indicated that both transformations were quantitative.

Preparation of (Cp*M$_1$(NO)(CH$_2$SiMe$_3$)](μ-N)[Cp*M$_2$(O)(CH$_2$SiMe$_3$) [M = Mo, W] (6). The $[(Cp^*M_1(NO)(CH_2SiMe_3)](\mu\text{-}N)[Cp^*M_2(O)(CH_2SiMe_3)]$ [M = Mo, W] complex was prepared in a manner analogous to that described for the Mo dimeric complexes **4** and **5** (vide supra). The only difference was that complexes **6** could be easily crystallized by cooling the final concentrated pentane filtrate to −30 °C overnight. As before, ^{1}H NMR spectroscopic monitoring confirmed that the conversion of **3** → **6** was quantitative.

Reaction of [Cp*Mo(CH$_2$CMe$_2$Ph)]$_2$(μ-NO)$_2$ (2) with L (L = Pyridine, PMe$_3$, PPh$_3$). These experiments were conducted in NMR tubes. The reaction of **2** with PPh_3 is given as a representative example. Complex **2** (20 mg, 0.030 mmol) was combined with an excess of PPh_3 (15 mg, 0.060 mmol) in C_6D_6 (0.8 mL). The ^{1}H NMR spectrum of the reaction mixture (recorded after 12 h) revealed peaks attributable to **5** and free PPh_3. In a similar way, complex **2** merely isomerized to complex **5** in the presence of an excess of either PMe_3 or pyridine.

Reaction of [Cp*Mo(CH$_2$CMe$_3$)]$_2$(μ-NO)$_2$ (1) with [Cp*Mo(CH$_2$CMe$_2$Ph)]$_2$(μ-NO)$_2$ (2). **1** (20 mg, 0.030 mmol) and **2** (24 mg, 0.030 mmol) were combined in C_6D_6 (0.8 mL) in an NMR tube. The ^{1}H NMR spectrum of the reaction mixture (recorded after 12 h) revealed peaks only attributable to complexes **4** and **5**.

Reaction of Molecular Hydrogen with a Mixture of Cp*Mo(NO)(CH$_2$CMe$_2$Ph)$_2$ and Cp*Mo(NO)(CH$_2$CMe$_3$)$_2$. A quantity of C_6H_6 (20 mL) was vacuum transferred onto a solid mixture of Cp*Mo(NO)(CH$_2$CMe$_2$Ph)$_2$ (264 mg, 0.5 mmol) and Cp*Mo(NO)(CH$_2$CMe$_3$)$_2$ (200 mg, 0.5 mmol), and then H_2 (1 atm) was introduced into the reaction vessel. The stirred reaction mixture was warmed slowly to room temperature over 20 min, during which time its color changed from red to green. The solvent was removed from the final reaction mixture in vacuo, and the resulting green-blue residue was washed with pentane (5 mL). The washed residue was then dissolved in Et_2O (30 mL) and transferred onto a column of Florisil (2 × 2 cm) supported on a medium-porosity frit. The column was washed with Et_2O (2 × 10 mL). The filtrate was then taken to dryness under reduced pressure, and the remaining residue was redissolved in a minimal amount of toluene. Cooling of the toluene solution at −30 °C overnight induced the formation of a blue powder. Parent peaks (m/z = 664, 788, 727) attributable to [Cp*Mo(CH$_2$CMe$_3$)]$_2$(μ-NO)$_2$ (**1**), [Cp*Mo(CH$_2$CMe$_2$Ph)]$_2$(μ-NO)$_2$ (**2**), and [Cp*Mo(CH$_2$CMe$_2$Ph)](μ-NO)$_2$[Cp*Mo(CH$_2$CMe$_3$)] were observed in the mass spectrum of this powder. No attempts were made to separate or further characterize these complexes.

Reaction of Cp*Mo(NO)(CH$_2$SiMe$_3$)$_2$ with Acetone or Benzaldehyde in the Presence of Molecular Hydrogen. The reaction of Cp*Mo(NO)(CH$_2$SiMe$_3$)$_2$ with H_2 and acetone is given as a representative example. H_2 was added (1 atm) to an evacuated reaction vessel containing a mixture of Cp*Mo(NO)(CH$_2$SiMe$_3$)$_2$ (410 mg, 0.94 mmol), acetone (0.1 mL, 1.4 mmol), and pentane (20 mL) at −78 °C. The stirred reaction mixture was warmed slowly to room temperature (1 h) during which time its color changed from purple to red. Solvent was removed in vacuo, and the reaction vessel was kept under vacuum for 2 h to obtain a red residue. This residue was redissolved in pentane (10 mL) and filtered through a column of Celite (3 × 3 cm) supported on a frit. The eluate was then concentrated under reduced pressure (3 mL). Cooling at −30 °C for 3 weeks did not induce crystallization, and thus the solvent was removed in vacuo for 12 h. The red residue was then redissolved in C_6D_6 (0.6 mL) and transferred into an NMR tube for spectroscopic characterization. The spectroscopic data was consistent with the residue being Cp*Mo(NO)(CH$_2$SiMe$_3$)(OCHMe$_2$) (~90% yield by ^{1}H NMR). Using benzaldehyde instead of acetone, Cp*Mo(NO)(CH$_2$SiMe$_3$)(OCH$_2$Ph) (~90% yield by ^{1}H NMR) was similarly obtained.[17]

Cp*Mo(NO)(CH$_2$SiMe$_3$)(OCHMe$_2$). ^{1}H NMR (C_6D_6): δ 5.22 (ses, 1H, OC*H*Me$_2$), 1.58 (s, 15H, C$_5$Me$_5$), 1.32 (d, 3H, OCH*Me*$_2$), 1.29 (d, 3H, OCH*Me*$_2$), 1.13 (d, 1H, CH$_2$, J_{HH} = 11.4 Hz), 0.85 (d, 1H, CH$_2$, J_{HH} = 11.4 Hz), 0.34 (s, 9H, SiMe$_3$). ^{13}C{^{1}H} NMR (C_6D_6): δ 113.2 (*C*$_5$Me$_5$), 82.7 (CH), 39.1 (*C*H$_2$SiMe$_3$), 28.5 (Me), 26.9 (Me), 10.2 (C$_5$*Me*$_5$), 2.5 (CH$_2$Si*Me*$_3$).

Cp*Mo(NO)(CH$_2$SiMe$_3$)(OCPhH$_2$). ^{1}H NMR (C_6D_6): δ 7.46 (m, 2H, Ph), 7.15 (m, 3H, Ph) 5.91 (m, 2H, OC*H*$_2$Ph), 1.42 (s, 15H, C$_5$Me$_5$), 1.31 (d, 1H, CH$_2$, J_{HH} = 9.9 Hz), 1.16 (d, 1H, CH$_2$, J_{HH} = 9.9 Hz), 0.40 (s, 9H, SiMe$_3$). ^{13}C{^{1}H} NMR (C_6D_6): δ 142.4 (OCH$_2$), 129.3 (C$_{ortho}$), 128.6 (C$_{meta}$), 127.8 (C$_{para}$), 112.9 (*C*$_5$Me$_5$), 42.0 (*C*H$_2$SiMe$_3$), 9.6 (C$_5$*Me*$_5$), 2.1 (CH$_2$Si*Me*$_3$). C$_{ipso}$ not observed.

Reaction of Cp*W(NO)(CH$_2$SiMe$_3$)$_2$ with Molecular Hydrogen. H_2 was added (1 atm) to an evacuated reaction vessel containing Cp*W(NO)(CH$_2$SiMe$_3$)$_2$ (100 mg, 0.19 mmol) and C_6H_6 (10 mL) at 5 °C. The stirred reaction mixture was warmed to room temperature (15 min) during which time no color change was noticed. The benzene was removed from the reaction mixture in vacuo, and the resulting purple residue was dissolved in pentane (~5 mL). Cooling of this solution at −30 °C overnight induced the formation of a purple crystals. The spectroscopic data of these crystals matched those of authentic Cp*W(NO)(CH$_2$SiMe$_3$)$_2$.

(17) The tungsten analogues, namely Cp*W(NO)(CH$_2$SiMe$_3$)(OCHMe$_2$) and Cp*W(NO)(CH$_2$SiMe$_3$)(OCH$_2$Ph), have been isolated as pure crystals. Debad, J. D.; Legzdins, P.; Lamb, S. A.; Batchelor, R. J.; Einstein, F. W. B. *Organometallics* **1995**, *14*, 2543.

Kinetic Measurements of the Conversion of [Cp*Mo(CH$_2$CMe$_2$Ph)]$_2$(μ-NO)$_2$ (2) to [(Cp*Mo(NO)(CH$_2$CMe$_2$Ph)](μ-N)[Cp*Mo(O)(CH$_2$CMe$_2$Ph)] (5). A sample of complex **2** (3 mg, 0.004 mmol) was weighed into a 10-mL volumetric flask (0.0004 M) in a drybox. The flask was filled with toluene and shaken. An aliquot was transferred to a 1.00-cm UV−vis spectrophotometer cell equipped with a 4-mm Teflon stopcock. The cell was placed in the cell holder of a Hewlett-Packard 8542A diode array spectrometer. The temperature of the cell holder was maintained constant (±0.1 °C) by a Haake W19 temperature bath equipped with a Haake D8 temperature controller or a VWR 9501-1156 temperature bath equipped with a digital temperature controller. The solution was left to equilibrate (300 s) with the temperature of the water bath before spectra were recorded. Spectra were then recorded at regular intervals, and data were collected for at least 3.5 half-lives. The absorbance values at infinity were computer optimized. The rate constants (k_{obsd}) were then calculated from plots of $\ln(A_t - A_\infty)$ versus time (in seconds). $\Delta H^\ddagger$ and $\Delta S^\ddagger$ were determined from the Eyring plot of $\ln(k_{obsd}/T)$ versus $1/T$ from which $\Delta H^\ddagger = -R$(slope) and $\Delta S^\ddagger = R$[intercept − $\ln(k_b/h)$], where R, k_b, and h are the gas constant, Boltzmann's constant, and Planck's constant, respectively.

X-ray Crystallographic Analyses of [Cp*Mo(CH$_2$CMe$_3$)]$_2$(μ-NO)$_2$ (1) and [Cp*M$_1$(NO)(CH$_2$SiMe$_3$)](μ-N)[Cp*M$_2$(O)(CH$_2$SiMe$_3$)] (6). X−ray quality crystals of **1** were obtained by slow cooling of a saturated toluene solution of the complex to −30 °C overnight. Single crystals of **6** were obtained as two polymorphs (**A** and **B**) by recrystallization of the analytically pure material from pentane and toluene, respectively. Under a dry dinitrogen atmosphere, crystal fragments of both complexes were cleaved and gently wedged (with a trace of Apiezon N grease as adhesive) into glass capillary tubes which were then hot-wire sealed. Data were recorded at 185 K for **1** and at ambient temperature (297 K) for **6** with an Enraf Nonius CAD4F diffractometer using graphite-monochromatized Mo Kα radiation and an in-house modified low-temperature attachment. Two standard reflections per hour were measured in each case and exhibited only small intensity variations (<±2%) for **1** and **6B**. However, those for **6A** showed a systematic decline in intensity totaling 22%. All data were corrected for absorption by the Gaussian integration method,[18] and the corrections were carefully checked against measured ψ scans. Data reduction included corrections for intensity scale variation and for Lorentz and polarization effects.

The programs used for absorption corrections, data reduction, structure solution, and graphical output were from the *NRCVAX* crystal structure system.[19] Refinement was carried out using the program suite *CRYSTALS*.[20] Complex scattering factors for neutral atoms[21] were used in the calculation of structure factors. In the final cycles of full-matrix least-squares refinement, weighting schemes were used for which $\langle w(|F_o| - |F_c|)^2\rangle$ was nearly constant as a function of both $|F_o|$ and sin θ/λ (based on counting statistics for **1** and **6B** and unit weights for **6A**). Computations were carried out on MicroVAX-II and 80486 computers. Crystallographic details are summarized in Table 4.

For complex **1**, coordinates and anisotropic thermal parameters for all non-hydrogen atoms were refined with all hydrogen atoms included in calculated positions 0.95 Å from their respective carbon atoms and with isotropic temperature factors initially proportionate to the carbon-atom equivalent isotropic temperature factors. The CH$_3$ groups of the Cp* ligand were refined as rigid groups subject to 15 soft restraints which maintained approximate axial symmetry for each CCH$_3$ fragment. A single isotropic temperature factor was refined for the hydrogen atoms of each Cp* methyl group and another for the methylene hydrogen atoms of the neopentyl group. The temperature factors for the methyl carbon atoms of the neopentyl group and electron-density difference maps indicated unequal conformational disorder of CMe$_3$. A second site was included in the refinement for each of these three methyl carbon atoms, initially subject to reasonable distance restraints which were later released. The relative occupancies of the two orientations

(18) Busing, W. R.; Levy, H. A. *Acta Crystallogr.* **1957**, *10*, 180.

(19) Gabe, E. J.; LePage, Y.; Charland, J.-P.; Lee, F. L.; White, P. S. NRCVAX − An Interactive Program System for Structure Analysis. *J. Appl. Crystallogr.* **1989**, *22*, 384.

(20) Watkins, D. J.; Carruthers, J. R.; Betteridge, P. W. CRYSTALS. Chemical Crystallography Laboratory, University of Oxford, Oxford, England, 1984.

(21) *International Tables for X-ray Crystallography*; Kynoch Press: Birmingham, England, 1975; Vol. IV, p 99.

Table 4. Crystallographic Data for the Structure Determinations of $[Cp^*Mo(CH_2CMe_3)](\mu\text{-}NO)_2$ (**1**) at 185 K and Two Polymorphs (**6A**,**B**) of $[Cp^*M_1(NO)(CH_2SiMe_3)](\mu\text{-}N)[Cp^*M_2(O)(CH_2SiMe_3)]$ (M_1, M_2 = Mo, W) (**6**) at 297 K

	1	**6A**	**6B**
formula	$Mo_2O_2N_2C_{30}H_{52}$	$WMoSi_2O_2N_2C_{28}H_{52}$	$WMoSi_2O_2N_2C_{28}H_{52}$
fw	664.63	784.69	784.69
cryst syst	orthorhombic	monoclinic	monoclinic
space group	*Pbcn*	$P2_1/n$	$P2_1/c$
a (Å)[a]	12.570(3)	17.402(2)	13.940(3)
b (Å)	15.566(2)	7.898(2)	19.953(3)
c (Å)	15.610(3)	25.910(4)	12.112(3)
β (deg)		101.74 (2)	97.99(2)
V (Å^3)	3054.3	3486.6	3336.2
T (K)	185	297	297
Z	4	4	4
ϱ_c (g cm^{-3})	1.445	1.495	1.562
λ (Mo Kα_1) (Å)	0.70930	0.70930	0.70930
μ(Mo Kα) (mm^{-1})	0.83	3.81	3.98
cryst dimens (mm)	0.25 × 0.33 × 0.35	0.24 × 0.34 × 0.40	0.17 × 0.24 × 0.28
trans[b]	0.794−0.830	0.362−0.499	0.506−0.562
2θ range	4−50	4−45	4−45
R_F[c]	0.025	0.047	0.029
R_{wF}[d]	0.030	0.050	0.037

[a] Cell dimensions were determined in each case from 25 reflections (**1**, 34° ≤ 2θ ≤ 46°; **6A**, 30° ≤ 2θ ≤ 39°; **6B**, 34° ≤ 2θ ≤ 42°). [b] The data were corrected by the Gaussian integration method for the effects of absorption. [c] $R_F = \sum||F_o| - |F_c||/\sum|F_o|$, for 1921 (**1**), 2735 (**6A**), and 3096 (**6B**) data ($I_o \geq 2.5\sigma(I_o)$). [d] $R_{wF} = [\sum(w(|F_o| - |F_c|)^2)/\sum(wF_o^2)]^{1/2}$ for observed data (see *c*, above); **1**, **6B**, $w = [\sigma(F_o)^2 + 0.0001F_o^2]^{-1}$; **6A**, $w = 1$.

(including recalculated hydrogen atoms for each component) were refined and constrained to total one. A single parameter was refined for the thermal motion of the three methyl carbon atoms of the minor conformation and another for all the hydrogen atoms of the disordered methyl groups. The hydrogen atoms of the neopentyl group were made to ride on their respective carbon atoms during refinement. Final full-matrix least-squares refinement of 196 parameters for 1921 data ($I_o \geq 2.5\sigma(I_o)$) converged at $R = 0.025$. The final maximum |shift/error| was 0.01, and the maximum peak in the final difference map was 0.28(7) e Å^{-3}. Final fractional atomic coordinates for the non-hydrogen atoms are given in the supporting information.

During the refinement of each of the structures **6A**,**B**, hydrogen atoms were included in calculated positions (d(C−H) = 0.95 Å) with appropriate occupancies and isotropic displacement parameters initially derived from the displacement parameters for the carbon atoms to which they were bound. The hydrogen atoms were made to ride on their respective carbon atoms during refinement, and where appropriate, the hydrogen-atom site occupancies were linked with those of their respective carbon atoms. When rigid-group refinement of disordered Cp* ligands was employed (**6A**), the appropriate hydrogen atoms were included in the groups. For **6B**, a single variable was refined for the isotropic displacements for each set of chemically equivalent hydrogen atoms and the shifts were applied to the individual hydrogen-atom displacement parameters. The hydrogen atoms of **6A** were treated similarly except that only two H-atom displacement variables were refined, one for the isotropic displacement of the hydrogen atoms of the CH_2SiMe_3 groups and another for that of the hydrogen atoms of the Cp* groups.

The asymmetric unit of **6A** consisted of one molecule disordered such that the two transition metal sites each had partial occupancy by both W and Mo while the oxo and nitrosyl ligands were disordered over the same coordination sites in a complementary fashion. Because of the similarity of the covalent radii for Mo and W, one set of coordinates and anisotropic displacement parameters was refined for each of the metal sites using partial contributions from the appropriate scattering factors. Independent relative occupancy parameters for each of the metal sites and for the NO/O disordered sites were included in the refinement while the M−N, M−O, and N−O bond distances and the M−N−O bond angles (M = W or Mo) were restrained to reasonable values obtained from the structures of analogous homometallic species.[22] The nearly overlapping fractional atoms of the nitrosyl and oxo groups were constrained to have the same isotropic displacement parameters. The resultant occupancies differed significantly from 0.5 and were consistent with the existence of two opposing orientations of a single diastereomer/conformer of the molecule having a possible formulation $[Cp^*W(NO)(CH_2SiMe_3)](\mu\text{-}N)[Cp^*Mo(O)(CH_2SiMe_3)]$. Subsequently, these individual relative occupancy parameters were replaced by a single parameter consistent with such an assumption. However, it is likely that the disorder also involved the structural isomers in which the NO or O ligands may be bonded to either molybdenum or tungsten as was found for polymorph **6B** (vide infra).

The CH_2SiMe_3 groups in **6A** were ordered, and anisotropic displacement parameters were included for the silicon atoms. The η^5-Cp* ligands, however, displayed rotational disorder about the metal atom to Cp*-centroid axis coupled with small lateral displacements. Each Cp* was ultimately refined as two fractionally occupied rigid groups with an isotropic atomic displacement parameter for each set of 10 chemically equivalent carbon-atom sites. The metal to C bonding distances for each MCp* fragment were restrained toward their mean value. The refined occupancies, constrained to total one for each pair of overlapping disordered groups, did not differ significantly from 0.5, and there was no secure basis for associating a particular Cp* orientation either with Mo or W metal-site occupation or with the nitrosyl- or oxo-ligand substitution.

Based upon observed electron-density difference map features, anisotropic displacement parameters for all the methyl carbon atoms and for one nearly coincident N/O disordered pair were included in the refinement subject to reasonable "null-motion" soft restraints. These were further constrained such that the N/O pair had a common set of atomic displacement parameters as did pairs of approximately opposing (across the center-of-mass of each disordered Cp*) methyl C atoms of the Cp* ligands. The final full-matrix least-squares refinement of 226 parameters for 2735 observations and 52 restraints converged (maximum |shift/esd| = 0.02) at $R = 0.047$. The largest features in the final difference map occurred 1.05 Å from W(1) (−1.3(2) e Å^{-3}) and 0.92 Å from W(2) (0.7(2) e Å^{-3}). Final fractional coordinates for the non-hydrogen atom sites are listed in the supporting information.

Polymorph **6B** also displayed disorder of the transition-metal sites, but the other atoms, most notably the NO and O ligands, were ordered! The transition metal sites were modeled similarly to those of **6A**. Anisotropic displacement parameters for the non-hydrogen atom sites and an extinction parameter[20] (0.09(3) μm) were refined. The final full-matrix least-squares refinement of 333 parameters for 3096 observations converged (maximum |shift/esd| = 0.01) at $R = 0.029$. The maximum peak in the final difference map (0.6(1) e Å^{-3}) occurred 1.18 Å from W/Mo(1). Final fractional coordinates for the non-hydrogen atoms are given in the supporting information.

(22) Larson, A. C. In *Crystallographic Computing*; Munksgaard: Copenhagen, Denmark, 1970; p 291.

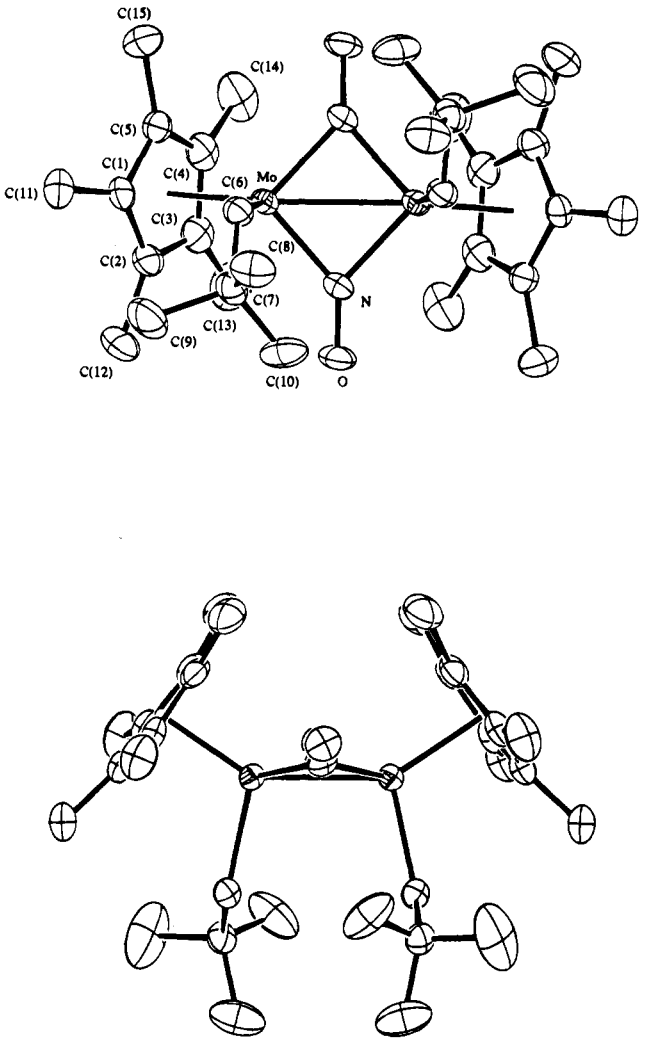

Figure 1. Two views of the solid-state molecular structure of $[Cp^*Mo(CH_2CMe_3)]_2(\mu\text{-}NO)_2$ (**1**). Ellipsoids of 50% probability are shown. Hydrogen atoms and the minor disordered components of the neopentyl groups have been omitted for clarity.

Results and Discussion

Formation of $[Cp^*MoR]_2(\mu\text{-}NO)_2$ Complexes. If the reaction of the bis(neopentyl) or bis(neophyl) complex $Cp^*Mo(NO)R_2$ (R = CH_2CMe_3 or CH_2CMe_2Ph) with H_2 (1 atm) in C_6H_6 is effected at 5 °C and the reaction mixture is worked up after 20 min, intermediate, thermally unstable blue complexes (**1** and **2**, respectively) are isolable in crystalline form in 26–33% yields. Elemental analysis indicates that the crystals of **1** and **2** have the molecular composition $Cp^*Mo(NO)R$, and low-resolution mass spectra display features which suggest that the complexes are dimeric. Consistently, ^1H and ^{13}C NMR spectra of the blue crystals exhibit only signals attributable to one Cp* and one R group, and their Nujol-mull IR spectra display absorptions attributable to ν_{NO} at 1332 (**1**) and 1339 cm^{-1} (**2**) in the region expected for η^2-NO or bridging NO ligands.[23] The solid-state molecular structure of **1** has been established by a single-crystal X-ray crystallographic analysis and is shown as an ORTEP diagram in Figure 1.

Solid-State Molecular Structure of $[Cp^*Mo(CH_2CMe_3)]_2(\mu\text{-}NO)_2$ (1). The crystal structure of **1** consists of the packing of discrete dimeric molecular units separated by normal intermolecular contact distances. The molecule (shown in Figure 1) has crystallographic 2 (*C*2) point symmetry. The NO groups bridge the two Mo atoms symmetrically, and the ON-$(Mo)_2$ fragment is approximately planar. There is a puckering of the MoN_2 core of the molecule such that the NO groups are inclined toward the Cp* side of the molecule, the dihedral angle between the two Mo_2N planes being 159.0 (1)°. The intramolecular dimensions of this bridging unit resemble those extant in $[CpCr(NO)]_2(\mu\text{-}NO)_2$,[24] $(CpFe)_2(\mu\text{-}NO)_2$,[25] and $[Cp^*RuCl]_2(\mu\text{-}NO)_2$.[26] For example, the N–O bond length in complex **1** is 1.259 (3) Å while that in $(CpFe)_2(\mu\text{-}NO)_2$ is 1.254 (12) Å. Selected bond lengths and bond angles for complex **1** are provided in Table 5. The Mo–N bond length is typical of that expected for a single bond.[27] An interesting feature of the molecular structure of **1** is the cis geometry of the Cp* groups, the Cp*–Mo–Mo′–Cp* torsion angle being −13.3°. This configuration is opposite to the trans geometry adopted by the $[CpCr(NO)]_2(\mu\text{-}NO)_2$ and $[Cp^*RuCl]_2(\mu\text{-}NO)_2$ complexes cited above. The most chemically interesting feature of the molecular structure of **1** is the Mo–Mo bond distance of 2.5930(7) Å, which is more consistent with the existence of a relatively short, single metal–metal bond[28] rather than a relatively long Mo≡Mo linkage.[29] Each metal center in **1** may thus be viewed as having a formal 16-valence-electron configuration. Curiously, complexes **1** and **2** (presumably isostructural with **1**) do not form adducts with simple Lewis bases such as phosphines or pyridine and their thermal conversions to complexes **4** and **5** (vide infra) are also not prevented by such bases.

Table 5. Selected Intramolecular Distances (Å) and Angles (deg) for Complex **1**

Mo–Mo′ [a]	2.5930(7)	Mo–C(6)	2.203(3)
Mo–N	1.944(3)	Mo–*Cp* [b]	2.055
Mo–N′	1.977(3)	O–N	1.259(3)
Mo–C(1)	2.458(3)	Mo–C(4)	2.337(3)
Mo–C(2)	2.413(3)	Mo–C(5)	2.379(3)
Mo–C(3)	2.334(3)		
Mo′–Mo–N	49.14(8)	N′–Mo–C(6)	109.10(11)
Mo′–Mo–N′	48.05(8)	N′–Mo–*Cp*	115.58
Mo′–Mo–C(6)	101.79(8)	C(6)–Mo–*Cp*	112.17
Mo′–Mo–*Cp*	146.02	Mo–N–Mo′	82.80(10)
N–Mo–N′	95.04(11)	Mo–N–O	138.52(21)
N–Mo–C(6)	102.06(11)	Mo′–N–O	138.16(21)
N–Mo–*Cp*	120.92	Mo–C(6)–C(7)	126.54(21)

[a] Prime symbols indicates the equivalent position (−*x*, *y*, 0.5 − *z*). [b] *Cp* denotes the center of mass of the carbon atoms of the cyclopentadienyl ring.

Formation of $[Cp^*Mo(NO)R](\mu\text{-}N)[Cp^*Mo(O)R]$ Complexes. Both complexes **1** and **2** isomerize in solutions within 2 h at ambient temperatures to the nitrido oxo bimetallic species $[Cp^*Mo(NO)R](\mu\text{-}N)[Cp^*Mo(O)R]$ (R = CH_2CMe_3 (**4**), R = CH_2CMe_2Ph (**5**)) in which the metal centers have attained the favored 18-valence-electron configurations (eq 2). To the best

(23) Richter-Addo, G. B.; Legzdins, P. *Metal Nitrosyls*; Oxford University Press: New York, 1992; Chapter 2.

(24) Calderón, J. L.; Fontana, S.; Frauendorfer, E.; Day, V. W. *J. Organomet. Chem.* **1974**, *64*, C10.

(25) Calderón, J. L.; Fontana, S.; Frauendorfer, E.; Day, V. W.; Iske, S. D. A. *J. Organomet. Chem.* **1974**, *64*, C16.

(26) Hubbard, J. L.; Morneau, A.; Burns, R. M.; Zoch, C. R. *J. Am. Chem. Soc.* **1991**, *113*, 9176.

(27) For examples of typical Mo–N single-bond lengths, see: (a) Shih, K.-Y.; Schrock, R. R.; Kempe, R. *J. Am. Chem. Soc.* **1994**, *116*, 8804. (b) Hughes, D. L.; Mohammed, M. Y.; Pickett, C. J. *J. Chem. Soc., Dalton Trans.* **1990**, 2013. (c) Dehniche, K.; Strähle, J. *Angew. Chem., Int. Ed. Engl.* **1992**, *31*, 955. (d) Noble, M. E.; Folting, K.; Huffman, J. C.; Wentworth, R. A. D. *Inorg. Chem.* **1982**, *21*, 3772.

(28) Silverthorn, W. E.; Couldwell, C.; Prout, K. *J. Chem. Soc., Chem. Commun.* **1978**, 1009.

(29) Cotton, F. A.; Walton, R. A. *Multiple Bonds Between Atoms*, 2nd ed; Oxford University Press: New York, 1993; Chapter 5.

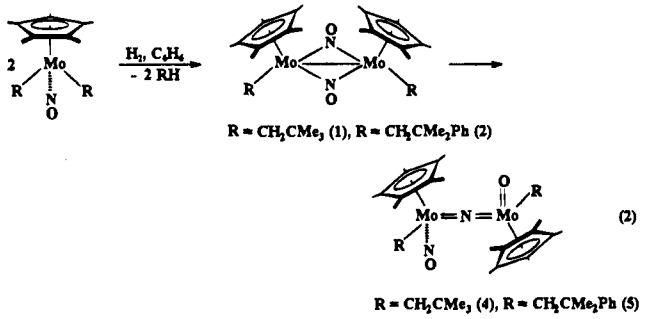

R = CH_2CMe_3 (1), R = CH_2CMe_2Ph (2)

R = CH_2CMe_3 (4), R = CH_2CMe_2Ph (5)

of our knowledge, these isomerizations involving the conversion of bridging nitrosyl ligands to their oxo and nitrido constitutents are unique.[30] Furthermore, they occur intramolecularly as evidenced by the fact that an equimolar mixture of **1** and **2** converts cleanly to an equimolar mixture of **4** and **5** upon warming (eq 3).[31]

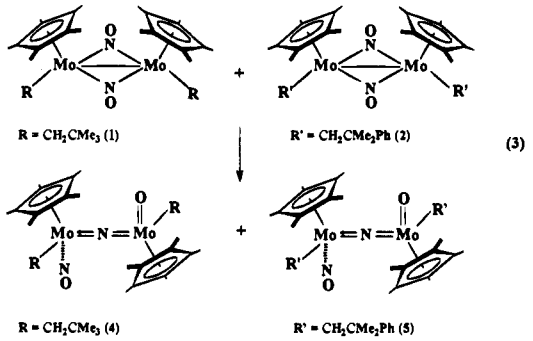

R = CH_2CMe_3 (1) R' = CH_2CMe_2Ph (2)

R = CH_2CMe_3 (4) R' = CH_2CMe_2Ph (5)

Kinetic Studies. UV−vis spectroscopy may be utilized conveniently to monitor the progress of the isomerization of **2** to **4**, since blue $[Cp^*Mo(CH_2CMe_2Ph)]_2(\mu\text{-}NO)_2$ (**2**) exhibits an absorbance at 684 nm in its UV−vis spectra while the brown oxo nitrido complex $[(Cp^*Mo(NO)(CH_2CMe_2Ph)](\mu\text{-}N)[Cp^*Mo(O)(CH_2CMe_2Ph)]$ (**4**) shows no features at this wavelength.

The isomerization of **2** to **4** in toluene in first order in **2** with k_{obsd} (20 °C) = 1.1 ± 0.3 × 10^{-4} s^{-1}.[32] The kinetic analysis was also affected at different temperatures, and Table 6 contains the observed rate constants (k_{obsd}) at 10, 20, 30, 40, and 50 °C in toluene. The initial concentration of $[Cp^*Mo(CH_2CMe_2Ph)]_2(\mu\text{-}NO)_2$ was maintained at 4 × 10^{-4} M (3 mg in 10 mL toluene) throughout. These rate constants and temperatures were used to construct the Eyring plot shown in Figure 2. $\Delta H^{\ddagger}$ was calculated from the plot to be 39 ± 3 kJ/mol, while $\Delta S^{\ddagger}$ was found to be −188 ± 6 J/mol K (−45 ± 3 cal/mol K). The high negative value of the entropy of activation implies a highly ordered transition state.[33] It is also consistent with the isomerizations occurring in an intramolecular manner (vide supra).

Reaction of H_2 with a Mixture of $Cp^*Mo(NO)(CH_2SiMe_3)_2$ and $Cp^*W(NO)(CH_2SiMe_3)_2$. Exposure of an equimolar mixture of $Cp^*Mo(NO)(CH_2SiMe_3)_2$ and $Cp^*W(NO)(CH_2SiMe_3)_2$ to H_2 results in the formation of the heterobimetallic species $[Cp^*Mo(CH_2SiMe_3)](\mu\text{-}NO)_2[Cp^*W(CH_2SiMe_3)]$ (**3**).

(30) A related fragmentation of a CO ligand occurs during thermolysis (120 °C for 4 h) of $[(silox)_2WCl(CO)]_2$, which affords the oxo-μ-carbido complex $(silox)_2(O)W{=}C{=}WCl_2(silox)_2$, see: Miller, R. L.; Wolczanski, P. T.; Rheingold, A. L. *J. Am. Chem. Soc.* **1993**, *115*, 10422.

(31) **1** (20 mg, 0.030 mmol) and **2** (24 mg, 0.030 mmol) were combined in C_6D_6 (0.8 mL) in an NMR tube. The ^1H NMR spectrum of the reaction mixture revealed after 12 h peaks only attributable to complexes **4** and **5**.

(32) Three or four kinetic runs were conducted for each temperature. The error limits were calculated using standard statistical methods: Gordon, A. J.; Ford, R. A. *The Chemist's Companion*; Wiley-Interscience: New York, 1972.

(33) Wood, C. D.; McLain, S. J.; Schrock, R. R. *J. Am. Chem. Soc.* **1979**, *101*, 3210.

Table 6. Rate Data

temp (°C)	rate const (s^{-1})	conc (M)[a]	mean rate const (s^{-1})[b]
10.0	7.6 × 10^{-5}	0.0004	
10.0	6.7 × 10^{-5}	0.0004	(6.8 ± 0.9) × 10^{-5}
10.0	7.2 × 10^{-5}	0.0004	
10.0	5.7 × 10^{-5}	0.0004	
20.0	1.0 × 10^{-4}	0.0004	
20.0	9.5 × 10^{-5}	0.0004	(1.1 ± 0.3) × 10^{-4}
20.0	1.2 × 10^{-4}	0.0004	
20.0	1.3 × 10^{-4}	0.0008	
20.0	1.1 × 10^{-4}	0.0013	
30.0	1.6 × 10^{-4}	0.0004	
30.0	1.9 × 10^{-4}	0.0004	(1.7 ± 0.3) × 10^{-4}
30.0	1.6 × 10^{-4}	0.0004	
40.0	3.5 × 10^{-4}	0.0004	
40.0	3.5 × 10^{-4}	0.0004	(3.3 ± 0.6) × 10^{-4}
40.0	2.9 × 10^{-4}	0.0004	
40.0	3.3 × 10^{-4}	0.0013	
50.0	4.3 × 10^{-4}	0.0004	
50.0	4.6 × 10^{-4}	0.0004	(4.8 ± 0.9) × 10^{-4}
50.0	5.4 × 10^{-4}	0.0004	

[a] Solvent is toluene. [b] Based on the rate constants measured at 0.0004 M (values for Eyring plot).

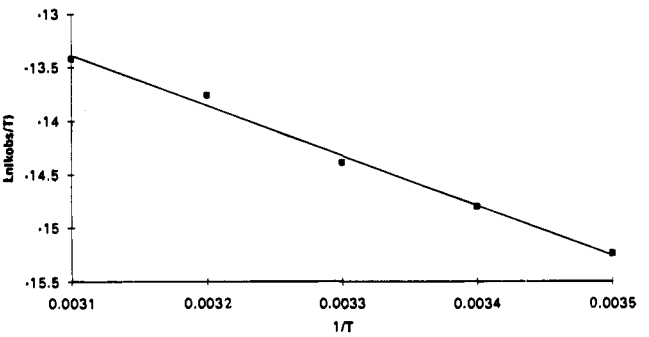

Figure 2. Eyring plot for the isomerization of $[Cp^*Mo(CH_2CMe_2Ph)]_2(\mu\text{-}NO)_2$ (**2**) to $[(Cp^*Mo(O)(CH_2CMe_2Ph)](\mu\text{-}N)[Cp^*Mo(NO)(CH_2CMe_2Ph)]$ (**4**) in toluene.

There is no evidence for the formation of the homonuclear bridging nitrosyl complexes viz. $[Cp^*Mo(CH_2SiMe_3)]_2(\mu\text{-}NO)_2$ or $[Cp^*W(CH_2SiMe_3)]_2(\mu\text{-}NO)_2$ during this transformation. The physical properties of **3** are consistent with it being analogous to complexes **1** and **2**. Hence, it is not surprising that complex **3** is thermally unstable in solutions and converts to **6**, which is a mixture of two structural isomers (eq 4) that are analogous to complexes **4** and **5** (vide supra).

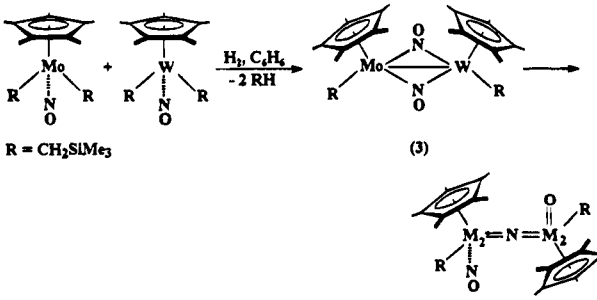

R = CH_2SiMe_3

(6; M_1 = W (60%), M_1=Mo(40%))

A single-crystal X-ray crystallographic analysis of **6** (described in the next section) has established that both structural isomers, namely $[Cp^*W(NO)(CH_2SiMe_3)](\mu\text{-}N)[Cp^*Mo(O)(CH_2SiMe_3)]$ (ca. 60%) and $[Cp^*Mo(NO)(CH_2SiMe_3)](\mu\text{-}N)[Cp^*W(O)(CH_2SiMe_3)]$ (ca. 40%), are present in the unit cell (Figure 3).

Solid-State Molecular Structure of Complex 6. Two differnt crystals of complex **6** (**6A,B**) were analyzed by X-ray

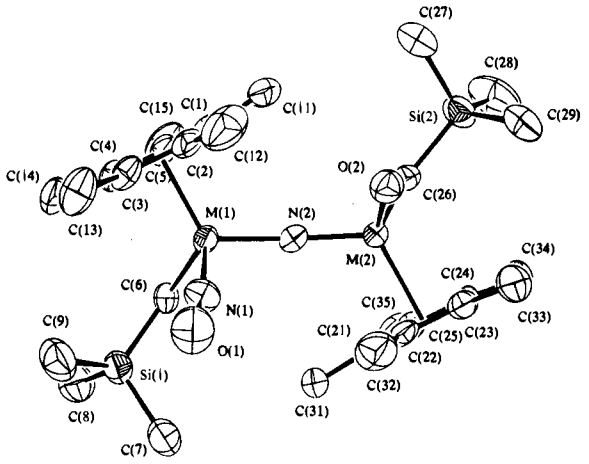

Figure 3. Solid-state molecular structure of [(Cp*M₁(O)(CH₂SiMe₃)](μ-N)[Cp*M₂(NO)(CH₂SiMe₃)] (**6**). Ellipsoids of 50% probability are shown, and the hydrogen atoms have been omitted for clarity.

Table 7. Selected Intramolecular Distances (Å) and Angles (deg) for Complex **6** (Polymorph **6B**)

W/Mo(1)−N(1)	1.770(7)	W/Mo(2)−O(2)	1.718(6)
W/Mo(1)−N(2)	1.913(7)	W/Mo(2)−N(2)	1.818(6)
W/Mo(1)−C(6)	2.174(7)	W/Mo(2)−C(26)	2.158(8)
W/Mo(1)−*Cp1*[a]	2.068	W/Mo(2)−*Cp2*[b]	2.115
W/Mo(1)−C(1)	2.396(10)	W/Mo(2)−C(21)	2.405(9)
W/Mo(1)−C(2)	2.281(9)	W/Mo(2)−C(22)	2.478(8)
W/Mo(1)−C(3)	2.358(9)	W/Mo(2)−C(23)	2.504(9)
W/Mo(1)−C(4)	2.454(8)	W/Mo(2)−C(24)	2.439(8)
W/Mo(1)−C(5)	2.453(9)	W/Mo(2)−C(25)	2.338(9)
Si(1)−C(6)	1.865(8)	Si(2)−C(26)	1.868(8)
Si(1)−C(7)	1.857(10)	Si(2)−C(27)	1.848(11)
Si(1)−C(8)	1.852(9)	Si(2)−C(28)	1.862(11)
Si(1)−C(9)	1.864(11)	Si(2)−C(29)	1.850(10)
O(1)−N(1)	1.194(10)		
N(1)−W/Mo(1)−N(2)	98.1(3)	W/Mo(1)−C(6)−Si(1)	122.7(4)
N(1)−W/Mo(1)−C(6)	97.1(3)	W/Mo(2)−C(26)−Si(2)	120.6(4)
N(1)−W/Mo(1)−*Cp1*	121.8	C(6)−Si(1)−C(7)	111.6(4)
N(2)−W/Mo(1)−C(6)	108.7(3)	C(6)−Si(1)−C(8)	109.3(4)
N(2)−W/Mo(1)−*Cp1*	118.0	C(6)−Si(1)−C(9)	114.8(4)
C(6)−W/Mo(1)−*Cp1*	110.7	C(7)−Si(1)−C(8)	108.4(5)
O(2)−W/Mo(2)−N(2)	106.6(3)	C(7)−Si(1)−C(9)	105.7(5)
O(2)−W/Mo(2)−C(26)	101.8(3)	C(8)−Si(1)−C(9)	106.8(5)
O(2)−W/Mo(2)−*Cp2*	117.8	C(26)−Si(2)−C(27)	110.4(4)
N(2)−W/Mo(2)−C(26)	103.3(3)	C(26)−Si(2)−C(28)	108.1(5)
N(2)−W/Mo(2)−*Cp2*	115.7	C(26)−Si(2)−C(29)	115.4(4)
C(26)−W/Mo(2)−*Cp2*	109.7	C(27)−Si(2)−C(28)	108.4(6)
W/Mo(1)−N(1)−O(1)	170.0(7)	C(27)−Si(2)−C(29)	107.1(5)
W/Mo(1)−N(2)−W/Mo(2)	157.3(4)	C(28)−Si(2)−C(29)	107.3(6)

[a] *Cp1* represents the center of mass of atoms C(1) through C(5). [b] *Cp2* represents the center of mass of atoms C(21) through C(25).

crystallography. The analysis of **6B** afforded the ORTEP shown in Figure 3 and the selected intramolecular bond angles and both lengths contained in Table 7. The investigation of the structure of polymorph **6B** was undertaken since the extensively disordered structure of **6A** did not permit the resolution of the question of the isomerism detected for **6** by ^{1}H NMR spectroscopy. The structural model for **6A**, in which both the transition-metal sites and the NO and O ligands are mutually disordered, can be interpreted in terms of a purely orientational disorder. In **6B** only the transition metals are disordered, a feature which leads to the conclusion that two structural isomers are present, namely [Cp*W(NO)(CH₂SiMe₃)](μ-N)[Cp*Mo(O)(CH₂SiMe₃)] (59.3%) and [Cp*Mo(NO)(CH₂SiMe₃)](μ-N)[Cp*W(O)(CH₂SiMe₃)] (40.7%). This conclusion is consistent with the ratio of isomers detected in solutions by ^{1}H NMR spectroscopy (Table 3).

The molecular structure deduced from the analysis of crystal **6B** displays a nearly linear M−N−M′ arrangement of 157.3-(4)°. There is also significant asymmetry in the bond lengths to the central nitrogen, i.e. W/Mo(1)−N(2) 1.913 (7) Å and W/Mo(2) 1.818 (6) Å, which is reasonably consistent with simple valency requirements for the two metal sites. These structural features are similar to those determined for the analogous structures [Cp*W(NO)(CH₂CMe₃)](μ-N)[Cp*W(O)(Cl)] and [Cp*Mo(NO)(CH₂SiMe₃)](μ-N)[Cp*Mo(O)(CH₂SiMe₃)].[11] Both crystals **6A,B** contain the same heterometallic diastereomers, namely the *R,S* species in which the Cp* groups are mutually anti (or trans), the Cp*−M−N−M′−Cp* torsion angle established from the analysis of **6B** being 177°. Interestingly, this *R,S* stereochemistry is opposite to that observed for the analogous homometallic structures mentioned above during whose formation intermediates analogous to **3** have not been detected.[11]

Mechanistic Ideas. A plausible mechanism for the first steps in the conversions shown in eq 2 involves the initial formation of an unstable molybdenum alkyl hydride, Cp*Mo(NO)(R)H, from the hydrogenolysis of the bis(alkyl) molybdenum reactant. This hydride can be trapped when Cp*Mo(NO)(CH₂SiMe₃)₂ is hydrogenated in the presence of acetone or benzaldehyde (see the Experimental Section). Also consistent with the view that the reaction progresses through a transient hydride is the fact that the hydrogenation of a mixture of Cp*Mo(NO)(CH₂CMe₃)₂ and Cp*Mo(NO)(CH₂CMe₂Ph)₂ produces a mixture of complexes **1**, **2**, and the mixed alkyl complex [Cp*Mo(CH₂CMe₃)](μ-NO)₂[Cp*Mo(CH₂CMe₂Ph)]. This hydride could next dimerize with concomitant loss of H_2,[34] thereby resulting in the nitrosyl ligands adopting bridging positions in order to satisfy some of the electronic unsaturation extant at the metal centers. The M(μ-NO)₂M bridging systems in these products could then cleave in the manner depicted below to form the final nitrido-bridged complexes **4** and **5**. The thermodynamic

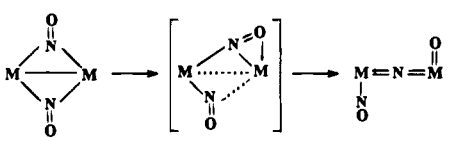

M = Cp*M'R (M' = Mo, W; R = CH_2SiMe_3, CH_2CMe_3, CH_2CMe_2Ph)

driving force of the isomerizations shown above in undoubtedly the formation of a strong M=O bond as well as a strong M−N−M linkage.[35] However, it is not yet clear why the two symmetrically bridging nitrosyl ligands suffer such dramatically different fates during the isomerizations. Such cleavage of nitrosyl groups to form nitrido and oxo ligands has been observed previously in metal nitrosyl clusters.[7a]

The reaction of Cp*Mo(NO)(CH₂SiMe₃)₂ and Cp*W(NO)(CH₂SiMe₃)₂ with H_2 probably involves initial formation of an unstable Mo alkyl hydride species which first forms an adduct with Cp*W(NO)(CH₂SiMe₃)₂ and then rapidly eliminates alkane[36] and rearranges to form complex **3**. It is unlikely that any Cp*W(NO)(CH₂SiMe₃)H is formed during this process since it is known that Cp*W(NO)(CH₂SiMe₃)₂ does not react very rapidly with H_2 (see the Experimental Section). Cleavage

(34) (a) Dinuclear H_2 elimination has been observed in the reaction of Os(H)(CO)₄Os(Me)(CO)₄ with Os(CO)₄(H)(Me) to produce the trinuclear complex Os₃(CO)₁₂(Me)₂: Norton, J. R. *Acc. Chem. Res.* **1979**, *12*, 139. (b) A decomposition pathway of trnsition metal hydride complexes involves the formation of bimetallic bridging hydride complexes which then lose H_2 and result in the formation of a metal−metal bond: M−H → M(μ-H)M−H → M−M + H_2. Crabtree, R. H. *Comp. Coord. Chem.* **1987**, *2*, 689.

(35) Hall, K. A.; Mayer, J. M. *J. Am. Chem. Soc.* **1992**, *114*, 1024.

(36) Labeling studies have shown that the osmium complex Os(CO)₄HMe decomposes with the reductive dinuclear elimination of methane to yield the bimetallic complex Os(H)(CO)₄Os(CO)₄OsMe; see ref 33a.

of one of the bridging nitrosyl ligands in the heterometallic complex **3** in the manner depicted above then results in the formation of the two isomers $[Cp^*M_1(NO)(CH_2SiMe_3)](\mu\text{-}N)[Cp^*M_2(O)(CH_2SiMe_3)]$ (**6**), the final oxo ligand ending up on either the Mo or W center. Furthermore, the fact that both heterobimetallic complexes which constitute **6** are formed as the *R,S* diastereomers exclusively is consistent with **3** being cisoidal in nature (as in the analogous homometallic complex **1**).

All the other bridging nitrosyl systems synthesized to date (e.g., $[CpCr(NO)]_2(\mu\text{-}NO)_2$, $(CpFe)_2(\mu\text{-}NO)_2$, and $[Cp^*Ru(Cl)]_2(\mu\text{-}NO)_2$ cited earlier as well as $(CpCo)_2(\mu\text{-}NO)_2$,[37] $[Cp^*Ru(\mu\text{-}NO)]_2$,[38] $[Cp^*Ru(Ph)]_2(\mu\text{-}NO)_2$,[38] and $[Cp^*Fe(\mu\text{-}NO)]_2$[39]) are examples of electronically saturated complexes. The bridging nitrosyl complexes discovered during this work (i.e., **1**, **2**, and **3**) are electronically unsaturated and undergo the unique isomerizations to nitrido oxo bimetallic complexes (i.e., **4**, **5**, and **6**).

(37) Brunner, H. *J. Organomet. Chem.* **1968**, *12*, 517.
(38) Chang, J.; Bergman, R. G. *J. Am. Chem. Soc.* **1987**, *109*, 4298.
(39) Lichtenberger, D. L.; Copenhaver, A. S.; Hubbard, J. L. *Polyhedron* **1990**, *9*, 1783.

Acknowledgment. We are grateful to the Natural Sciences and Engineering Research Council of Canada for support of this work in the form of grants to P.L. and F.W.B.E., and we thank the University of British Columbia for the award of a University Graduate Fellowship to M.A.Y.

Supporting Information Available: Tables of hydrogen-atom coordinates, anisotropic thermal parameters, complete tables of bond lengths and bond angles, torsion angles, intermolecular contacts, and least-squares planes for complex **1** and both polymorphs of complex **6** (31 pages). This material is contained in many libraries on microfiche, immediately follows this article in the microfilm version of the journal, can be ordered from the ACS, and can be downloaded from the Internet; see any current masthead page for ordering information and Internet access instructions.

JA9437159